A validation study of OpenFOAM using the supersonic flow in a mixed compression intake

N M Sudharsan[1]*, **V A Jambekhar**[1], and **V Babu**[2]
[1]Sarvajit-CAE, Chennai, India
[2]Department of Mechanical Engineering, IIT Madras, Chennai, India

The manuscript was received on 5 July 2009 and was accepted after revision for publication on 18 November 2009.

DOI: 10.1243/09544100JAERO651

Abstract: The study of high-speed flows is of great importance in the design and manufacture of aerospace vehicles, missiles, and rockets. The flow physics is complex and experimental investigations with full size prototypes are quite expensive. To study such complex flows, there is a need for a numerical test bench that is both robust and customizable. To this end, in this study, a systematic validation of the open source computational fluid dynamics software called OpenFOAM has been undertaken. Numerical simulations of the high-Mach-number supersonic flow in a mixed compression intake in nine different configurations have been carried out. The predictions are seen to compare well with the experimental data reported in the literature. Important features such as the location and strength of oblique shocks and expansion fans are predicted well. The shock–boundary layer interaction for subtle variations in geometric configurations could also be replicated as observed experimentally. The roll up of the boundary layer due to shock interaction over very small time instants could be easily captured, which would be difficult do accomplish experimentally. Although not all permutations and combinations of the parameters have been studied, with the limited study the power of the above mentioned open source software has been established.

Keywords: high-speed flows, shock-boundary layer interaction, open source computational fluid dynamics software

1 INTRODUCTION

The study of high-speed supersonic flows with shock and boundary layer interaction is of great importance in aerospace applications. There is renewed interest in high-speed civil transport vehicles. Propulsion systems for such vehicles have to be designed for their operation at the subsonic, transonic, and high supersonic flight speeds. Practically, it is prohibitively expensive to build and test many prototype propulsion systems. However, numerical simulations can be effectively used for parametric studies and design evaluations, thus obviating the need for expensive fabrication and testing of all models. Although there are several commercial computational fluid dynamics (CFD) software available today, the objective of the present work is to evaluate an open source CFD package, namely Open Field Operations and Manipulation (OpenFOAM). Being an open source tool, it is attractive and provides the analyst with greater flexibility in customization. The facility to 'peep into the code' leads to a better understanding of the numerical schemes used, which is of importance in research. It also makes it possible to tailor the code for special applications. In this work, the code is used to study the 2D, non-reacting compressible flow in a supersonic intake, intended for use in a hypersonic air-breathing vehicle.

The shock–boundary layer interaction is seen, for example, in the intake of supersonic and hypersonic vehicles. Experimental and numerical results for such interactions are presented in references [**1**] to [**4**]. The objective of the present work, as mentioned earlier, is to carry out numerical simulations of the flow in a supersonic intake using OpenFOAM.

OpenFOAM [**5**] is a programmable toolkit. It is supplied with a source code and compilers. Customized

*Corresponding author: Sarvajit-CAE, 12, 5th Street, B.V. Nagar, Adyar, Chennai 600 020, India.
email: sudharsann@sarvajit-cae.com

applications are created for specific problems. Different functionalities are built into generic libraries (modules) to solve for different flow physics. Solid dynamics, pre-/post-processing, mesh generation, are also well supported by OpenFOAM. It has been used as a tool for research-oriented activities by numerous academic and research institutes. As it is open source software, users can customize the code for tighter tolerances. The present study is an effort to validate the performance of OpenFOAM for predicting the shock–boundary layer interaction in a mixed compression supersonic intake. For this evaluation, the inlet configurations investigated experimentally by Schneider and Koschel [**6**] are considered. The predictions from OpenFOAM are compared with the experimental data reported by Schneider and Koschel [**6**] and also the numerical data reported by Sivakumar and Babu [**7**]. However, as a first step, the propagation of shock for a flow over an inclined ramp is studied with OpenFOAM and compared with the results obtained by Oliver *et al.* [**8**]. Although several solvers are available in OpenFOAM for solving high-speed compressible flows, sonicTurboFoam has been chosen here, since viscous effects can be modelled, contrary to the other solvers. In addition it has the option to include turbulence models such as the k–ε, RNG (renormalization) k–ε, and realizable k–ε models. Yakhot *et al.* [**9**] showed that the RNG k–ε model is appropriate for the high-speed flow under consideration. Hence, the RNG k–ε model with wall functions is used in the present study.

2 VALIDATION

As mentioned earlier, a preliminary validation study of an oblique shock from a compression corner of angle 16° has been carried out (Fig. 1). The free stream Mach number, stagnation temperature, and stagnation pressure were 2.85, 268 K, and 6.8 bar, respectively [**8**]. A structured grid was created for this geometry using an OpenFOAM delivered meshing subroutine *blockMesh*. For this configuration, structured grids with 80 000, 165 000, 330 000, and 670 000 cells were created. It was found that predictions using the mesh with 330 000 cells compared well with the experimental results as discussed below. The maximum value for wall y^+ on this mesh was 55.

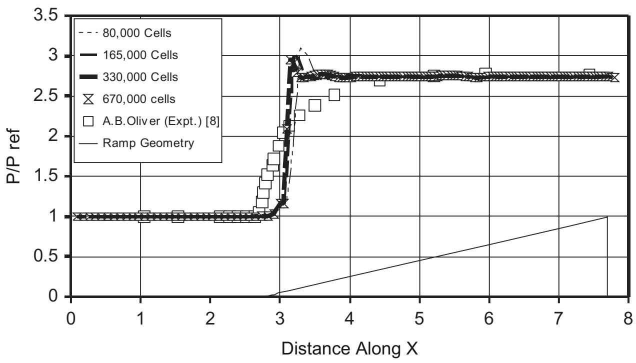

Fig. 1 Variation of P/Pref along the ramp surface for a compression corner

The finite volume discretization schemes used in the present calculations are as follows:

(a) time scheme: Euler time marching;
(b) gradient scheme: Gaussian;
(c) divergence scheme: u: Gauss linear, k: Gauss upwind, ε: Gauss upwind, p: Gauss linear;
(d) Laplacian schemes: Gaussian linear;
(e) interpolation scheme: linear.

The variation of wall static pressure P, non-dimensionalized with the inlet reference pressure, Pref, on the ramp surface is shown in Fig. 1. Predictions from the present study are compared with the experimental and computational results reported by Oliver *et al.* [**8**]. It can be seen that the predictions of OpenFOAM match well with the experimental results both ahead and behind the shock wave. However, the present calculations show a sudden rise in pressure as the supersonic air stream hits the ramp surface, in contrast to the experimental data, which shows a smooth increase. Furthermore, an overshoot is also seen immediately after the sharp rise. This overshoot does not diminish with further mesh refinement as is evident from Fig. 1. As mentioned earlier, the scheme used for divergence is Gauss linear. The numerical behaviour for this scheme is linear, second order, unbounded. The other option available is first order upwind. Although convergence was better in the latter case, comparison of the prediction with experimental data was poor. For this reason the second-order scheme without any upwinding was chosen. The lack of upwinding is the reason for the overshoot immediately downstream of the shock wave. It can also be seen from Fig. 1 that the predictions obtained using the grids with 330 000 and 670 000 cells did not differ.

3 NUMERICAL SET-UP

The supersonic mixed compression intake investigated by Schneider and Koschel [**6**] has been identified as an appropriate validation problem for evaluating the capability of OpenFOAM to predict such complex flows. The intake geometry is shown in Fig. 2, and the geometric details of the three configurations A, B, and C, for both the ramp and the cowl that have been simulated in the present work, are given in Table 1. A total of nine combinations of the ramp and cowl configurations have been simulated. It should be noted that locations 3 and 4 are varied for the ramp side and locations 6 and 7 are varied for the cowl side.

The geometry of the supersonic intake under investigation is shown in Fig. 2. The supersonic free stream ($M = 3$, $T_0 = 310$ K, and $P_0 = 0.15$ bar) is first

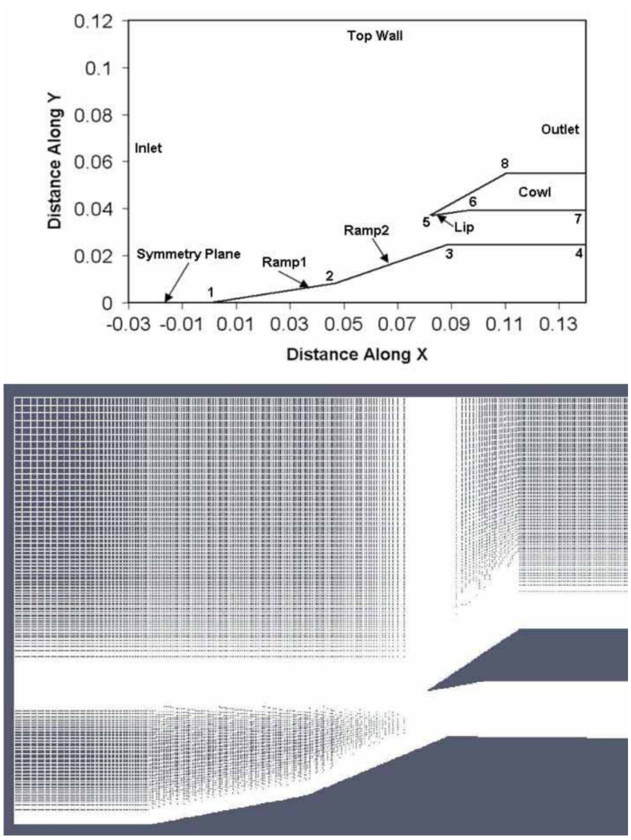

Fig. 2 Geometry and computational domain for the mixed compression intake [**8**] (see Table 1 for details)

Table 1 Model geometry configuration [**6**]

	X (mm)	Y (mm)	Location
Ramp			
A, B, and C	0	0	1
A, B, and C	46.73	8.24	2
A	88.8	24.81	
B	92.04	26.08	3
C	95.27	27.36	
A	125.79	24.49	
B	129.03	25.76	4
C	132.26	27.03	
Cowl			
A, B, and C	81.63	37.00	5
A	95.64	39.32	
B	100.46	40.15	6
C	105.45	40.98	
A	142.45	39.32	
B	142.45	40.15	7
C	142.45	40.98	
A, B, and C	110.00	55.00	8

compressed through oblique shocks generated from the corners of the ramp surface and then through reflected shocks in the internal passage. The C–C configuration (Ramp C and Cowl C) was also numerically simulated by Sivakumar and Babu [**7**] using Fluent. They had used an unstructured mesh with 119 098 cells, having a wall $y^+ < 30$. The simulation was carried out using the k–ε model with standard wall functions and the second-order upwinding scheme. Since this combination C–C has both the experimental and prior numerical results, it has been used for validating the OpenFOAM code. The unsteady, finite volume solver available in OpenFOAM has been used to obtain the steady-state solution and all calculations are first-order accurate in time and second-order accurate in space.

For accurately capturing the flow physics for high-speed flows, a wall y^+ value below 100 is desirable [**10**]. Thus adequate care was taken while generating the grid to ensure a very fine grid along the boundaries. Four meshes with 120 000, 180 000, 210 000, and 400 000 cells were generated to establish the grid independence of the results. It was observed that grid-independent results were obtained on the mesh with 210 000 cells as compared to 119 098 obtained using Fluent [**7**]. The maximum value for the wall y^+ on this mesh is 25. This mesh has been used for all other configurations except for the configuration C–A. Here, the mesh had to be refined further to achieve a wall y^+ value below 4 as it was observed to be a critical configuration [**6**]. This configuration will be discussed in detail later.

3.1 Boundary conditions

The boundary conditions and free stream parameters used for various geometric combinations are as presented in the chart below. The inlet, outlet, and wall boundary conditions specified in Table 2 are implemented for a numerical analysis of all the combinations used for evaluating OpenFOAM.

Fixed value: the value for the transported quantity, Φ, is fixed.

Inlet outlet: switches U and p between fixed value and zero gradient depending on the direction of u.

Zero gradient: the normal gradient for Φ is zero.

Slip: zero gradient if Φ is a scalar; if Φ is a vector, the normal component is fixed value zero, tangential components are zero gradient.

Table 2 Boundary conditions

	u	p	T	k	E
Inlet	Fixed value	Fixed value	Fixed value	Fixed value	Fixed value
Outlet	Inlet outlet	Wave transmission	Inlet outlet	Inlet outlet	Inlet outlet
Wall	Fixed value	Zero gradient	Zero gradient	Zero gradient	Zero gradient
Top wall	Slip	Zero gradient	Zero gradient	Zero gradient	Zero gradient
Bottom	Symmetry plane	Symmetry plane	Symmetry plane	Symmetry plane	Symmetry plane

Symmetry plane: the symmetry plane condition specifies the component of the gradient normal to be zero.

The Courant–Friedrichs–Lewy (CFL) number was in the range of 0.1–0.3. It required very low time stepping of the order of 5×10^{-7} s and was run for 24 s by which time the steady state was achieved. The time taken for the simulations on an average was about 21 650 s (6 h approximately). The machine used was an Intel Core 2 Duo at 2.00 GHz and 4 GB of RAM, running on OpenSUSE 11 OS.

The computational domain for the mixed compression intake configuration used in the present study is shown in Fig. 2. The velocity, temperature, and pressure (based on free stream conditions) are specified at the left boundary. The outlet boundary condition is set as free stream, i.e. in OpenFOAM parlance *Inlet Outlet*. The bottom wall is set as *Symmetry plane* in order to exploit the geometric symmetry. The ramp and the cowl surface are modelled as fixed walls with no slip (standard wall functions). The upper side of the computational domain is kept far enough to avoid any interaction with the shock generated by the upper portion of the cowl.

4 RESULTS AND DISCUSSION

In this section, comparison of the results obtained using OpenFOAM with the experimental data is presented and discussed for the nine intake configurations. The results for the C–C configuration are presented first, since numerical results [**7**] are also available for this configuration [**6**]. The variation of the static pressure along the surface of the ramp and the cowl for this configuration is presented in Figs 3 and 4, respectively. Contours of the dimensionless static pressure are shown in Fig. 5. The pressure rise is mainly caused by the first and the second ramp. The first ramp is inclined at 10°, whereas the second ramp is inclined at 15°. The oblique shocks generated from these corners decelerate and compress the air. The sudden decrease in pressure at the entry to the internal passage is caused by the expansion fan at this location. However, this drop in pressure is restricted by the oblique shock generated from the concave portion of the cowl. This is visible in Fig. 5 as well. It can be seen from Fig. 4 that there is a sudden increase in pressure as the shock generated by the second ramp hits the concave surface of the cowl. The pressure attains a peak value at the point where the tapered portion of the cowl lip ends (seen as a red contour patch at $x = 0.11$ m in Fig. 5). The pressure starts to decline further downstream, but increases again as the oblique shock from the ramp surface ($x = 0.14$ m) hits the cowl. It can also be seen from Figs 3 and 4 that the present results agree reasonably well with the experimental [**6**] and earlier numerical [**7**] results. However, there are oscillations behind the shock waves and the present results clearly fail to pick up the separation zone at the base of the compression corners.

From Fig. 5, it is noted that there is a low-pressure region at the expansion fan on the ramp shoulder (convex corner), which causes a sudden increase in the local Mach number. This low-pressure region is controlled by the incident shock wave that originates from

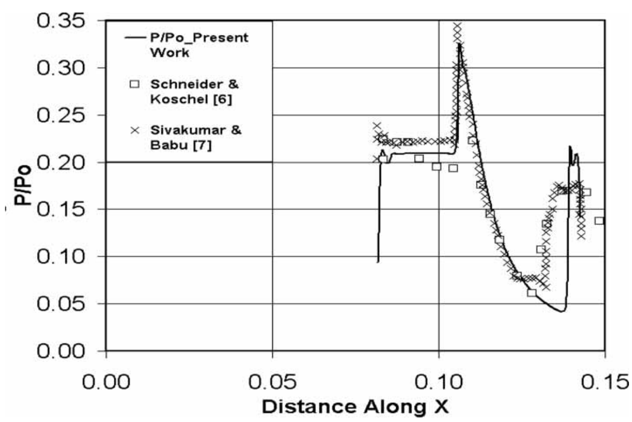

Fig. 4 Variation of P/Po on the inner surface of the cowl

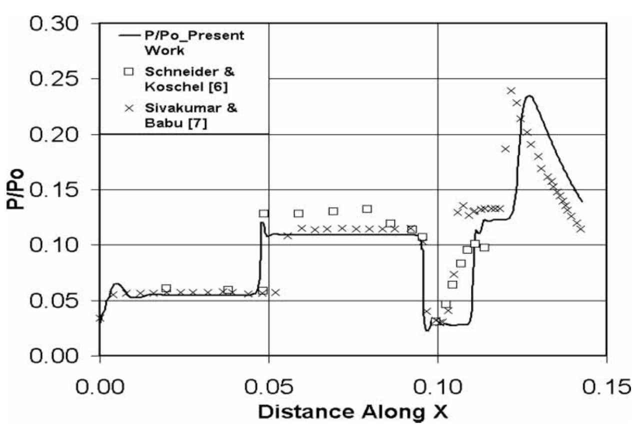

Fig. 3 Variation of P/Po on the ramp

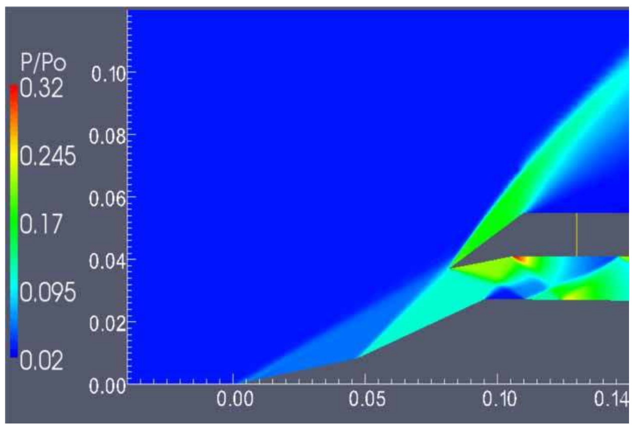

Fig. 5 P/Po for the CC ramp–cowl configuration

the cowl lip, hits the ramp boundary layer and tries to move underneath the boundary layer. This is seen as an increase in the pressure immediately after the expansion fan.

Schneider and Koschel [**6**] had mentioned that the C–A configuration was a critical configuration and hence the numerical predictions for this configuration need to be examined further. To this end, the grid for this configuration was refined until the final value for the wall y^+ was <5. Since the sublayer itself is resolved, wall functions have been dispensed with for this case.

The oblique shock generated from the cowl lip hits the ramp boundary layer further downstream when compared to the other configurations. The shock hits the ramp boundary layer immediately after the convex corner of the ramp and then rolls back. Figure 6 presents snapshots of the non-dimensional static pressure for the above configuration at different instants in time. The change in the location of the shock impingement point and also the reduction in the width of the low-pressure band located at the tip of the expansion fan at various intervals can be seen in these snapshots. As the shock hits the ramp further downstream, the pressure trough at the convex corner of the ramp seen in the other configurations near $x = 0.10$ m is completely absent now (Fig. 7). Comparing the present numerical results with those obtained experimentally, it can be seen that the present study slightly underpredicts the pressure for configuration C–A.

Figure 8 shows the variation of P/Po on the inner surface of the cowl. The present calculations predict a plateau near $x = 0.1$ m in contrast to the experimental data. The secondary peak seen in the experimental results near $x = 0.12$ m is also predicted by the calculations.

It can be seen from Fig. 9 that the low-pressure band around the expansion fan is lifted due to shock–boundary layer interaction. It was reported in the case of configurations C–A that the oblique shock from the cowl lip directly hits the ramp immediately after the

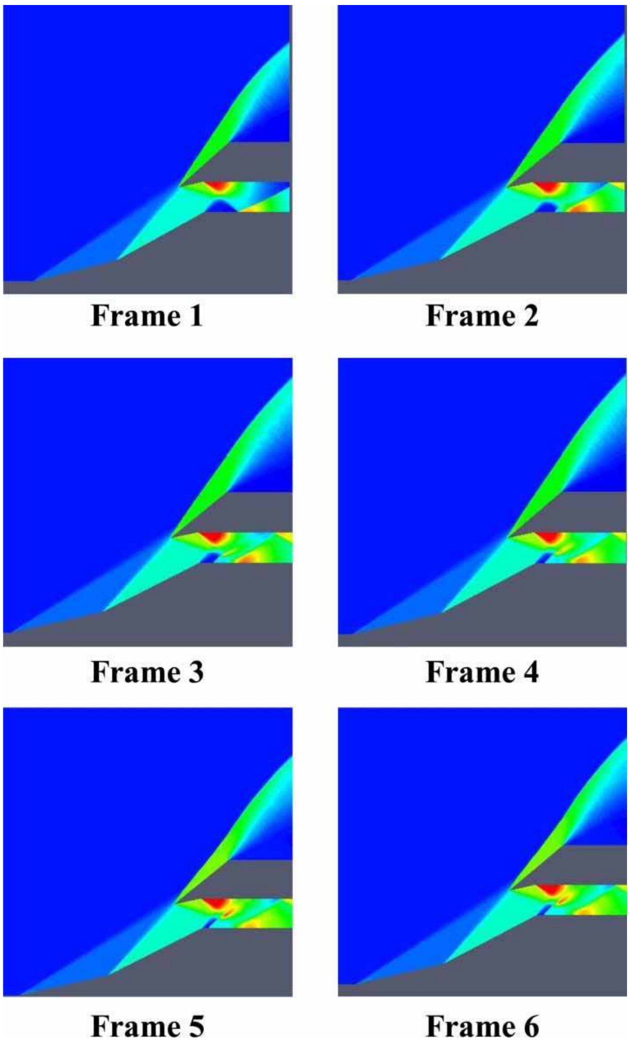

Fig. 6 Snapshots of P/Po for the C–A configuration at different instants in time

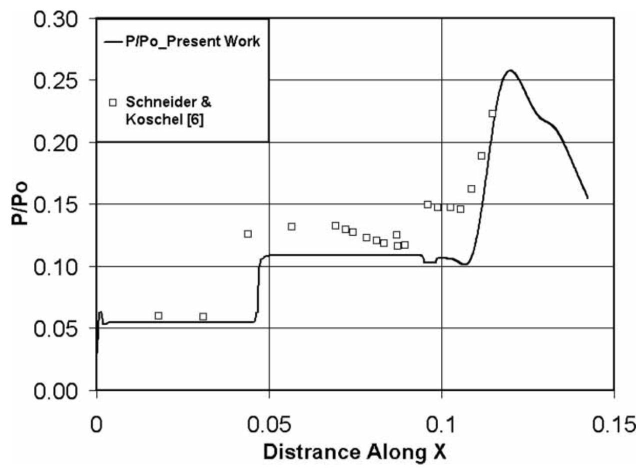

Fig. 7 Variation of P/Po on the ramp (C–A)

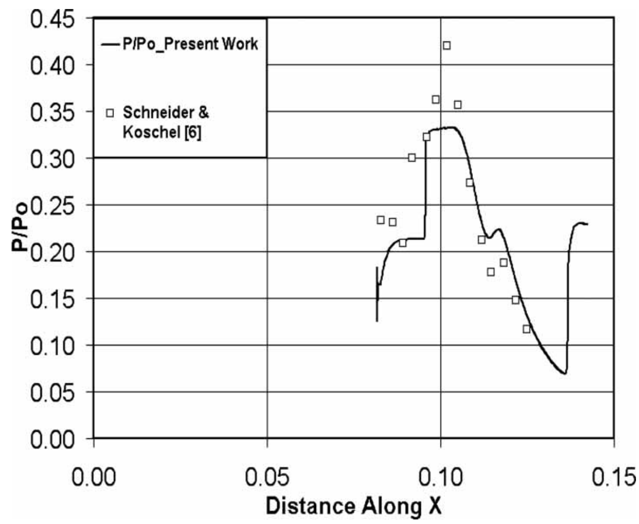

Fig. 8 Variation of P/Po on the inner surface of the cowl (C–A)

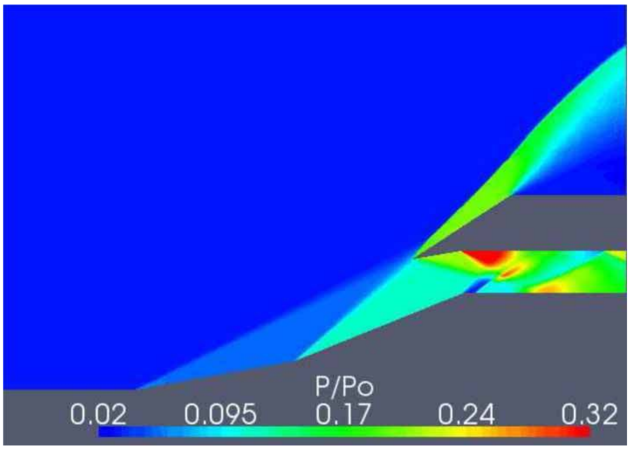

Fig. 9 Variation of P/Po for the ramp–cowl configuration (C–A)

convex corner and eliminates the low-pressure band [**6**]. However, with the validation using OpenFOAM it has been observed that the oblique shock hits the ramp surface after the expansion fan and gradually rolls back over time, squeezing this low-pressure band region until it reaches a steady state and not by directly hitting the expansion fan region as observed in reference [**6**]. It also attempts to move under the low-pressure region, thereby lifting the boundary layer. This roll back of the shock wave after it interacts with the ramp boundary layer can be clearly observed in Fig. 6.

Further validation of the numerical predictions with the experimental data reported by Schneider and Koschel [**6**] for a few more configurations given in Table 1 is presented in Figs 10 to 13. For all the cases compared, the predictions of OpenFOAM agree well with the experimental results. The variation of the dimensionless wall static pressure on the ramp and the inner surface of the cowl is shown in Figs 10 and 11 for configurations A–C. The initial pressure rise at the concave portion of the cowl was completely suppressed in the experiment for configurations A–C [**6**]. However, the current study predicts a slight pressure

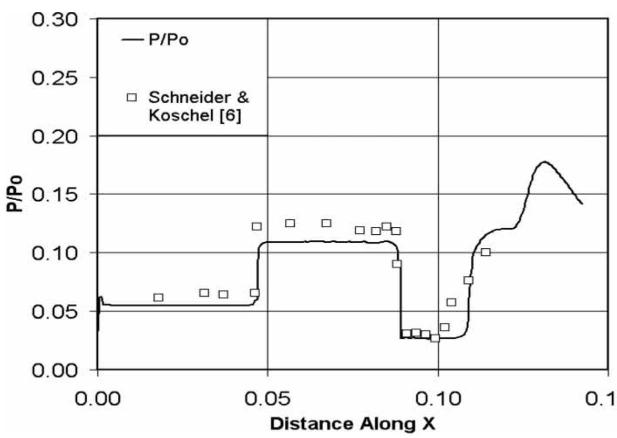

Fig. 10 Variation of P/Po on the ramp (A–C)

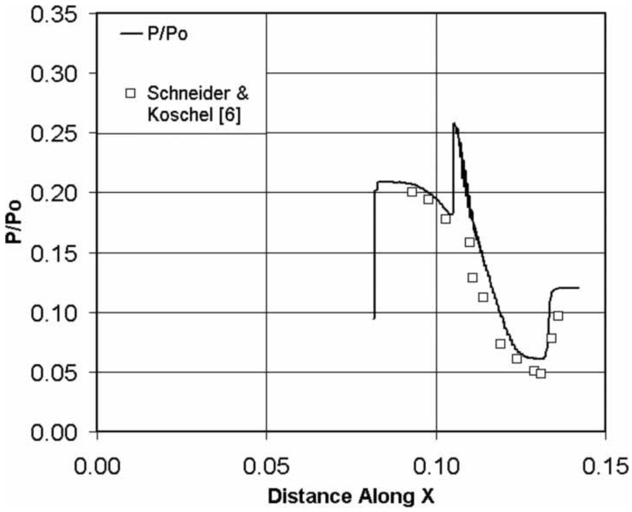

Fig. 11 Variation of P/Po on the cowl (A–C)

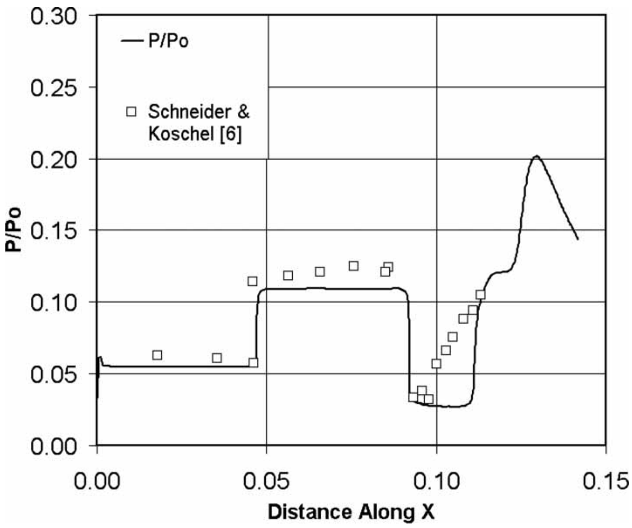

Fig. 12 Variation of P/Po on the cowl (B–C)

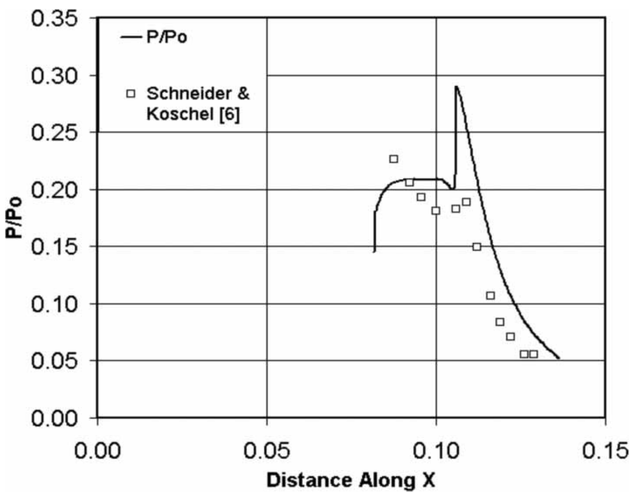

Fig. 13 Variation of P/Po on the cowl (B–C)

rise (Fig. 11). The pressure rise further downstream due to the recompression caused by the reflected shock waves is predicted well.

The variation of the dimensionless wall static pressure along the ramp and cowl inner surface for configurations B–C is shown in Figs 12 and 13. Once again, it can be seen that, except for the pressure rise near $x = 0.11$, the computational results obtained using OpenFOAM compare well with the experimental results.

5 CONCLUDING REMARKS

A systematic validation of the predictions of high-speed flows using OpenFOAM has been successfully attempted. The problem chosen for this validation study is the flow in a mixed compression supersonic intake [**6**]. It is well known that the flow field in such configurations is greatly affected by the configuration and even a small variation in the geometry will have a significant influence. This demands a high fidelity in the numerical calculations. The capability of OpenFOAM to capture the flow physics for all the configurations with reasonable accuracy without any additional customizations is clearly demonstrated by comparing the predictions with experimental data available in the literature [**6**]. Although the comparison of the predictions with experimental data is encouraging, undesirable features such as oscillations ahead of and behind shock waves are still present and need to be addressed.

Although some inferences on shock–boundary layer interaction could be drawn from the experiments, the numerical calculations can be carried out with very small time steps to understand the transient behaviour of the shock–boundary layer interaction. The time step used in this simulation was of the order of 10^{-7} s. Conducting a physical experiment to capture the flow physics with such a temporal resolution is at present extremely difficult if not impossible.

The critical C–A configuration required a resolution with a wall y^+ value of 4, resulting in a rather long computational time. Fine-tuning the CFD code with wall functions can help in solving such problems with a more lenient wall y^+, thus ensuring faster turnaround without loss of accuracy. More simulations by varying the angle of attack and supersonic and subsonic flows is necessary to make a critical review of the software to see if it can fully replace existing commercial software, which are expensive.

REFERENCES

1 **Holder, D. W., Pearcy, H. H.,** and **Gadd, G. E.** The interaction between shock waves and boundary layers. ARC technical report, 1955.

2 **Green, J. E.** Interactions between shock waves and turbulent boundary Layers. *Prog. Aerosp. Sci.*, 1970, **11**, 253–340.

3 **Watson, E. C., Rose, W. C., Morris Jr, S. J.,** and **Gallo, W. F.** Studies of the interaction of a turbulent boundary layer and a shock wave at Mach numbers between about 2 and 10. In Proceedings of the NASA Conference on *Hypersonic aircraft technology*, NASA SP-216, 1969, pp. 315–344, available from http://ntrs.nasa.gov/.

4 **Humble, R. A., Scarano, F.,** and **Van Oudheusden, B. W.** Experimental study of an incident shock wave/turbulent boundary layer interaction using PIV. AIAA paper 2006-3361, 2006.

5 OpenFOAM user Guide [online reference guide], OpenCFD, available from http://foam.sourceforge.net/doc/Guides-a4/UserGuide.pdf, United Kingdom.

6 **Schneider, A.** and **Koschel, W. W.** Detailed analysis of a mixed compression hypersonic intake. In Proceedings of the 14th International Symposium on *Air breathing engines* (*ISABE*), Florence, Italy, 5–10 September 1999 (AIAA, Reston, Virginia, USA).

7 **Sivakumar, R.** and **Babu, V.** Numerical simulations of flow in a 3-D supersonic intake at high Mach numbers. *Def. Sci. J.*, 2006, **56**(4), 465–476.

8 **Oliver, A. B., Lillard, R. P., Blaisdell, G. A.,** and **Lyrintzis, A. S.** Validation of high-speed turbulent boundary layer and shock-boundary layer interaction computations with the OVERFLOW code. AIAA paper 2006-0894, 2006.

9 **Yakhot, V., Orszag, S. A., Thangam, S., Gatski, T. B.,** and **Speziale, C. G.** Development of turbulence models for shear flows by a double expansion technique. *Phys. Fluids A*, 1992, **4**(7), 1510–1520.

10 **Rajasingh, T. G., Subash, C. B. S., Babu, V.,** and **Sundararajan, T.** Numerical investigation of the intake flow characteristics for a ramjet engine with and without heat addition in the combustion chamber. *Def. Sci. J.*, 2004, **54**(1), 3–16.